Clinical & Experimental Immunology
The Journal of Translational Immunology

Clinical and Experimental Immunology ORIGINAL ARTICLE doi:10.1111/j.1365-2249.2011.04452.x

Negative regulation of inflammatory responses by immunoglobulin A receptor (FcαRI) inhibits the development of Toll-like receptor-9 signalling-accelerated glomerulonephritis

T. Watanabe,* Y. Kanamaru,* C. Liu,* Y. Suzuki,* N. Tada,† K. Okumura,‡ S. Horikoshi* and Y. Tomino*

Department of Internal Medicine, Division of Nephrology, Juntendo University Faculty of Medicine, †Juntendo University Research Institute for Diseases of Old Ages, and ‡Juntendo University Atopy Research Center, Tokyo, Japan

Accepted for publication 21 June 2011
Correspondences: Y. Tomino, Division of Nephrology, Department of Internal Medicine, Juntendo University Faculty of Medicine, 2-1-1, Hongo, Bunkyo-ku, Tokyo, 113-8421, Japan.
E-mail: yasu@juntendo.ac.jp

Summary

Myeloid FcαRI, a receptor for immunoglobulin (Ig)A, mediates cell activation or inhibition depending on the type of ligand interaction, which can be either multivalent or monovalent. Anti-inflammatory signalling is triggered by monomeric targeting using anti-FcαRI Fab or IgA ligand binding, which inhibits immune and non-immune-mediated renal inflammation. The participation of Toll-like receptors (TLRs) in kidney pathology in experimental models and various forms of human glomerular nephritis has been discussed. However, little is known about negative regulation of innate-immune activation. In the present study, we generated new transgenic mice that express $Fc\alpha RI_{R209L}$/FcRγ chimeric protein and showed that the monovalent targeting of FcαRI exhibited inhibitory effects in an *in vivo* model of TLR-9 signalling-accelerated nephritis. Mouse monoclonal anti-FcαRI MIP8a Fab improved urinary protein levels and reduced the number of macrophages and immunoglobulin deposition in the glomeruli. Monovalent targeting using MIP8a Fab attenuates the TLR-9 signalling pathway and is associated with phosphorylation of extracellular signal-related protein kinases [extracellular signal-regulated kinase (ERK), P38, c-Jun N-terminal kinase (JNK)] and the activation of nuclear factor (NF)-κB. The inhibitory mechanism involves recruitment of tyrosine phosphatase Src homology 2 domain-containing phosphatase-1 (SHP-1) to FcαRI. Furthermore, cell transfer studies with macrophages pretreated with MIP8a Fab showed that blockade of FcαRI signalling in macrophages prevents the development of TLR-9 signalling-accelerated nephritis. These results suggest a role of anti-FcαRI Fab as a negative regulator in controlling the magnitude of the innate immune response and a new type of anti-inflammatory drug for treatment of kidney disease.

Keywords: animal models/studies – mice/rats, antibody responses, Fc receptors(FcRs), renal immunology/disease, signalling/signal transduction

Introduction

Chronic inflammatory disease results from continuous injuries or errors in regulatory control mechanisms [1,2]. An important control mechanism for the immune system is the inhibition of activating immunoreceptor tyrosine-based activation motif (ITAM)-bearing immunoreceptors, such as B and T lymphocyte antigen receptors, and the activation of Fc receptors by co-aggregating immunoreceptor tyrosine-inhibitory motif-bearing (ITIM) inhibitory receptors such as FcγRIIB and killer cell inhibitory receptors (KIR) [3]. This co-aggregation mechanism allows tyrosine phosphorylation of the ITIM by the kinases associated with the activating receptor. This leads to the recruitment of phosphatases, such as Src homology 2 (SH2) domain-containing phosphatase-1 (SHP-1) or SH2 domain-containing inositol phosphatase-1 (SHIP-1), to the phosphorylated ITIM. These phosphatases are then ideally localized to allow them to find their respective substrates and be recruited to the activating receptor or plasma membrane to impede ITAM-initiated signalling, including activation of kinases, adapter proteins or specific membrane effector recruitment.

Human CD89 (FcαRI), which is not expressed in rodents, is found on the surface of myeloid cells, including monocytes/macrophages, neutrophils and eosinophils, and binds to both IgA1 and IgA2. FcαRI is expressed

simultaneously with or without physical association with the FcRγ-chain homodimer [4,5]. FcαRI plays a role in a variety of inflammatory diseases via its powerful proinflammatory function. Recently, we reported that FcαRI and its associated FcRγ subunit exhibit a novel anti-inflammatory function for homologous immunoreceptors [6]. Inhibitory cross-talk was dependent on the FcRγ inhibitory ITAM (iITAM); it occurred without co-aggregation and was triggered after monomeric targeting of FcαRI with anti-FcαRI (A77) fragment antigen-binding (Fab) or immunoglobulin (Ig)A ligand binding. Similar to ITIM-mediated signals, down-regulation of the response involved the association of receptors with the tyrosine phosphatase SHP-1. Such dual receptor functions have since been observed for other ITAM-bearing receptors, including several innate immune receptors [7,8], suggesting that they might represent a widespread mechanism of immune regulation.

Recent discovery of the family of Toll-like receptors (TLRs) has focused attention on the disease processes, as TLRs mediate pathogen recognition and immune activation [9,10]. Bacterial DNA has been shown to be a pathogen-derived structure that activates the innate immune system through TLR-9 [11]. This activity depends on unmethylated cytosine-guanine dinucleotides (CpG), in particular base contexts [CpG oligodeoxynucleotides (CpG-ODNs)] [12]. Recently, it has been shown that CpG-ODNs induce nuclear factor (NF)-κB activation, p38 phosphorylation, extracellular signal-regulated kinase (ERK) and the synthesis and release of tumour necrosis factor (TNF)-α in macrophages [13]. TLR-mediated immune activation may play a role in immune complex diseases of the kidney triggered by infections. Horse apoferritin-induced glomerulonephritis (HAF-GN) is a model of immune complex GN that is characterized by circulating HAF-specific antibodies, mesangioproliferative GN, glomerular macrophage accumulation and proteinuria [14]. Single 40-μg doses of CpG DNA administered in the intraperitoneal cavity on days 7 and 8 (HAF-CpG-GN) led to a marked increase in the number of glomerular macrophages, the extent of glomerular damage and proteinuria [15]. Furthermore, analysis of serum anti-HAF antibody isotypes, mesangial immune deposits and splenocyte interferon (IFN)-γ, monocyte chemoattractant protein-1 (MCP-1) and regulated upon activation normal T cell expressed and secreted (RANTES) secretions indicated that CpG-DNA induced a T helper type 1 (Th1) response in mice with HAF-GN.

Previously, we reported that monovalent targeting of FcαRI strongly inhibited the development of immune complex-induced GN through decreased macrophage infiltration [16]. Therefore, we hypothesized that FcαRI targeting should control the harmful immune complex HAF-CpG-GN model mediated by TLR-9 signalling. We found that monomeric occupancy of FcαRI alleviated the worsening glomerular damage triggered by TLR-9 activation. These results suggest that shifting the inflammatory balance by specifically targeting FcαRI could represent a new viable option for the treatment of severe renal inflammatory diseases.

Materials and methods

Animals

The mice were bred and maintained in the mouse facilities of the Research Institute for Diseases of Old Age (Juntendo University School of Medicine, Tokyo, Japan). All experiments were conducted in accordance with national guidelines.

Obtaining a construct, generation of $Fc\alpha RI_{R209L}$/FcRγ transgenic (Tg) mice and preparation of the $Fc\alpha RI_{R209L}$/FcRγ transfectant

A construct encoding human $Fc\alpha RI_{R209L}$/FcRγ-FLAG was obtained by inserting a 1165-base pairs (bp) cDNA fragment into the *Escherichia coli* strain RI (EcoRI) site of a CAG promoter containing β-actin (UniTeck, Kashiwa, Japan). Three progeniture lines were found to contain the human $Fc\alpha RI_{R209L}$/FcRγ-FLAG cDNA by polymerase chain reaction (PCR) of tail DNA using transgene-specific primers 5 9-GGGTCATTAGTTCATAGCC-3 9 and 5 9-GGCATAT GATACACTTGAT- 3 9. The C57BL/6J background was introduced into line 604 by more than eight consecutive crosses. All mouse strains in this study were bred and housed in strictly controlled specific pathogen-free conditions. We prepared the $Fc\alpha RI_{R209L}$/FcRγ transfectant (I3D) from a mouse macrophage cell line (RAW264·7) using the Cell Line Optimization Nucleofector Kit (Lonza, Walkersville, MD, USA).

Cells and cell lines, culture and analysis of FcαRI (CD89) expression

The mouse macrophage cell line RAW264·7 was cultured in Glutamax (Invitrogen, Carlsbad, CA, USA) supplemented with 10% fetal calf serum (FCS), 100 U/ml penicillin and 100 μg/ml streptomycin at 37°C with 5% CO_2 in a humidified incubator. Stable transfectants in the presence of Geneticin (1·0 mg/ml; Sigma-Aldrich Chemicals, Steinheim, Germany) were selected.

Immunoglobulins and antibodies

The following antibodies were used: anti-FcaRI MIP8a Fab (affinity-purified monoclonal mouse anti human CD89 antibody (AbD Serotec, Oxford, UK)), human IgA (Jackson Immunoresearch Laboratories, West Grove, PA, USA), human IgG (Jackson), mouse monomeric IgA (BD Biosciences Pharmingen, San Diego, CA, USA), mouse polymeric IgA (Bethyl Laboratories, Montgomery, TX, USA), anti-FLAG (Rockland, Philadelphia, PA, USA), anti-syk (Santa Cruz Biotechnology, Santa Cruz, CA, USA), rabbit

anti-phospho ERK mitogen-activated protein kinases (MAPKs) p38 and c-Jun N-terminal kinase (JNK) antibodies (Cell Signaling Technology, Danvers, MA, USA), anti-phosphotyrosine monoclonal antibody (mAb) (4G10; Millipore, Billerica, MA, USA), rabbit anti-SHP-1 (Santa Cruz), anti-human CD16 Fab (Abbiotec, San Diego, CA, USA), anti-human CD32b Fab (Novus Biologicals, Littleton, CO, USA), anti-human CD64 Fab (R&D Systems, Minneapolis, MN, USA), goat anti-mouse IgM fluorescein isothiocyanate (FITC) and goat anti-mouse IgG rhodamine (Jackson), rat anti-mouse F4/80 antibody (AbD Serotec) and anti-SH-PTP1 antibody (Santa Cruz) were used.

Fluorescence activated cell sorter (FACS) analysis

Cells were incubated with fluorescent mAbs at 4°C for 1 h, then washed twice in phosphate-buffered saline (PBS) containing 2·0% fetal bovine serum (FBS) and fixed in 1·0% paraformaldehyde. Data were collected using FACSCalibur (BD Biosciences), and data analysis was performed using CellQuest software (BD Biosciences).

DNA extraction and PCR

$Fc\alpha RI_{R209L}$/FcRγ Tg mice genomic DNA was extracted from mouse tails. PCR was performed using puRe*Taq* Ready-To-Go PCR Beads (Amersham Bioscience, Amersham, UK).

Induction of HAF-CpG-GN

The following groups were studied. In group 1, mice received 80 μl normal saline once daily intraperitoneally. In group 2, mice were injected with 4 mg of horse spleen apoferritin (HAF; Sigma Aldrich Chemicals) in 80 μl of 0·1 M sodium chloride once daily intraperitoneally for 14 consecutive days. Mice in this group received 100 μl of normal saline intraperitoneally at 8 h after the HAF injection at days 7 and 8. In group 3, HAF was administered once daily as above. At days 7 and 8, 40 μg of endotoxin-free CpG-ODN 1668 (Invitrogen) in 100 μl of saline was administered intraperitoneally. In group 4, HAF was administered once daily as above. At days 7 and 8, 20 μg of MIP-8a in 200 μl of saline was administered via the caudal vein after 40 μg of endotoxin-free CpG-ODN administered intraperitoneally. In group 5, HAF was administered once daily as above. At days 7 and 8, 20 μg of control IgG in 200 μl of saline was administered via the caudal vein after CpG-ODN intraperitoneally. At day 14, samples and renal tissues were collected.

Biochemical data (urinary albumin and chemokine assays) and enzyme-linked immunosorbent assay (ELISA)

Urine samples were collected at days 0, 7, 9 and 14 in the morning. Urinary albumin was measured by immunoassay (DCA 2000 system; Bayer Diagnostics, Elkhart, IN, USA). Measurement of albuminuria is useful for detection of beginning of glomerular injury. This occurs before increasing of blood urea nitrogen (BUN) or creatinine values that sometimes mean renal failure. Blood samples were collected from each mouse at the end of the study from the retro-orbital venous plexus under general anaesthesia with inhaled ether. TNF-α, MCP-1 and RANTES levels were measured by ELISA (R&D Systems), according to the manufacturer's protocol.

Morphological analysis and immunohistochemical Staining

For light microscopy, the sections were cut at 3 μm and then stained with periodic acid-Schiff (PAS) reagent after paraffin embedding. The glomerular lesions were evaluated using a semiquantitative scoring method described previously [17]. The cell proliferation index was calculated using the following formula. For immunofluorescence and immunohistochemical staining the mouse kidneys were assessed on frozen 3-μm sections after −20°C acetone fixation and blocked by incubation with blocking solution [PBS (pH 7·2) containing 2·0% bovine serum albumin (IBSA), 2·0% FCS and 0·2% fish gelatin] for 60 min. Histological features were graded and $F4/80^+$ cells were counted blindly. A minimum of 50 equatorially sectioned glomeruli were assessed per animal. Results were expressed as cells/glomerular cross-section (/gcs), which was quantified using the KS-400 version 4·0 image analysis system (KS-400; Carl Zeiss Vision, Munich, Germany).

Immunoglobulin and immune complex preparation

Serum total IgG levels were measured by ELISA (mouse IgG ELISA Quantitation Kit; Bethyl Laboratories). Serum samples containing immune complexes (IC) were precipitated with an equal volume of 3·8% polyethylene glycol 6000 (PEG; Wako, Osaka, Japan) [16].

Cell isolation and adoptive transfer

FcαRI/FcRγ Tg spleen-derived macrophages were purified with anti-CD11b immunomagnetic beads (Miltenyi Biotec, Bergisch Gladbach, Germany); 2×10^6 of the monocytes/macrophages were injected into the lateral tail vein of each C57BL/6J mouse before injection of CpG.

Western blot analysis

Briefly, cultured cells were washed twice with ice-cold PBS and solubilized by incubation at 4°C for 15 min in lysis buffer (50 mM HEPES (pH 7·4), 0·3% Triton X-100, 50 mM NaF, 50 mM NaCl, 1 mM Na_3VO_4, 30 mM $Na_4P_2O_7$, 50 U/ml aprotinin and 10 μg/ml leupeptin). The protein concentration of the soluble extracts was determined using a protein

assay kit (Bio-Rad, Hercules, CA, USA). Collected samples were mixed with sample buffer (312·5 mmol/l Tris-HCl, pH 6·8, 10% SDS, 50% glycerol, 10% 2-mercaptoethanol and 0·025% bromophenol blue), heated at 95°C for 5 min before electrophoresis, resolved by sodium dodecyl sulphide-polyacrylamide gel electrophoresis (SDS-PAGE) using 10% acrylamide gel and transferred to polyvinylidene difluoride (PVDF) membranes. The blots were then performed as described previously [16].

NF-κB/AP-1 activity assay

Plasmid DNA (NF-κB-Lux or AP-1-Lux) was added to the I3D cells which were then detected using lipofectamine transfection reagent (Invitrogen) according to the manufacturer's instructions. At 72 h after transfection, 5 mM CpG stimulation was performed for 10 min after preincubation with anti-FcαRI Fab or control Fab (10 μg/ml for 12 h) and then lysed [Tris-HCl (pH 7·0–8·0), 2 mM dithiothreitol (DTT), 2 mM *trans*-1,2 diaminocyclohexanetetraacetic acid (CDTA) (pH 7·0), 10% glycerol, 1% TritonX, 4 mM $MgCl_2$, 4 mM ethyleneglycol tetraacetic acid (EGTA), 0·2 mM phenylmethylsulphonyl fluoride (PMSF)]. Luciferase activities were determined using Dual Luciferase Assay reagents (Promega, Fitchburg, WI, USA) according to the manufacturer's instructions.

Immunoprecipitation and tyrosine phosphorylation assay

Cells were immunoprecipitated with anti-SHP-1 antibody plus Protein G Sepharose 4 Fast Flow (Amersham), as described previously [6]. SHP-1 activities of the immunoprecipitated samples were measured by the Sensolyte pNPP protein phosphatase assay kit (Anaspec Corporate Headquarters, San Jose, CA, USA).

Data presentation

All experiments were repeated more than three times and representative results are shown. Data are expressed as mean ± 2 standard errors (s.e.). Statistical analyses were performed using Student's unpaired *t*-test (specifically for immunoblotting determination, we compared with each respective control) and analysis of variance (ANOVA). *P*-values of less than 0·05 indicated a statistically significant difference.

Results

Establishment of $Fc\alpha RI_{R209L}$/FcRγ chimeric transgenic mouse and RAW264·7 transfectant generation of human $Fc\alpha RI_{R209L}$/FcRγ Tg mice

A potent inhibitory ITAM (iITAM) signalling triggered by monovalent targeting of FcαRI requires an associated FcRγ chain. Transfectants expressing a R209L transmembrane FcαRI mutant that cannot associate with the FcRγ chain elicited neither inhibitory nor activating responses. To evaluate the precise role of FcαRI/FcRγ, we generated three Tg mouse lines with C57BL/6J backgrounds and designated them as 503, 505 and 604 using a construct containing human full-length $Fc\alpha RI_{R209L}$ cDNA, mouse FcRγ subunit and FLAG-tag under the control of the CAG promoter [18] (Fig. 1a). Macrophages isolated from the peripheral blood of C57BL/6J-Tg mice expressed $Fc\alpha RI_{R209L}$/FcRγ (Fig. 1b). Macrophage $Fc\alpha RI_{R209L}$/FcRγ expression was stable in 6–24-week-old mice (data not shown). The level of transgene expression was ~10-fold higher in macrophages from line 604 than from the other two lines (Fig. 1b). An example of a PCR assay demonstrating the simultaneous presence of human FcαRI DNA is shown in Fig. 1c. Analysis of protein extracts and sections from the peripheral blood in $Fc\alpha RI_{R209L}$/FcRγ Tg mice by Western blotting and staining with anti-FLAG antibody demonstrated the presence of a full-length 74-kDa human $Fc\alpha RI_{R209L}$/mouse FcRγ chimeric protein in $Fc\alpha RI_{R209L}$/FcRγ Tg mouse serum (Fig. 1c). The existence of soluble FcαRI was analysed using serum from aged $Fc\alpha RI_{R209L}$/FcRγ Tg because soluble FcαRI formed an immune complex with mouse IgA that led to IgA deposition in the glomeruli and nephropathy. As shown in Fig. 1d,e, there was no particularly soluble FcαRI band in $Fc\alpha RI_{R209L}$/FcRγ Tg mouse serum. Figure 1f,g shows that polymeric mouse IgA binds weakly to FcαRI and is sufficient to induce strong negative signals, whereas huge complexes such as soluble FcαRI/ mouse polymeric IgA induced aggregation of the receptor, which led to activation signals in the $Fc\alpha RI_{R209L}$/FcRγ transfectants (I3D).

FcαRI targeting reduces leucocyte infiltration and renal damage in mice with HAF-CpG-GN

To determine whether monovalent targeting of anti-FcαRI (MIP8a Fab) might have therapeutic implications for HAF-CpG-GN, we analysed the effect of MIP8a Fab treatment in HAF-CpG-GN mouse models of kidney disease. Mice treated with PBS or an unrelated control IgG developed elevated proteinuria, BUN and creatinine levels (Fig. 2a,b and not shown). Albuminuria was significantly attenuated in mice treated with MIP8a Fab (Fig. 2a). There were no significant differences in BUN and creatinine levels (Fig. 2b, not shown). Histological analysis of MIP8a Fab-treated animals also revealed markedly less glomerular expansion and hypercellular changes (Fig. 3a,c). PBS- or control IgG-treated animals had significantly high $CD11b^+/F4/80^+$ macrophage infiltration in glomeruli and interstitial tissue (Fig. 3b,d) after injection of CpG-ODN. However, MIP8a Fab-treated Tg mice showed decreased infiltration of $CD11b^+/F4/80^+$ macrophages in glomeruli and interstitial tissue compared with PBS- or control IgG-treated animals. Thus, MIP8a Fab treatment showed marked efficacy against HAF-CpG-GN.

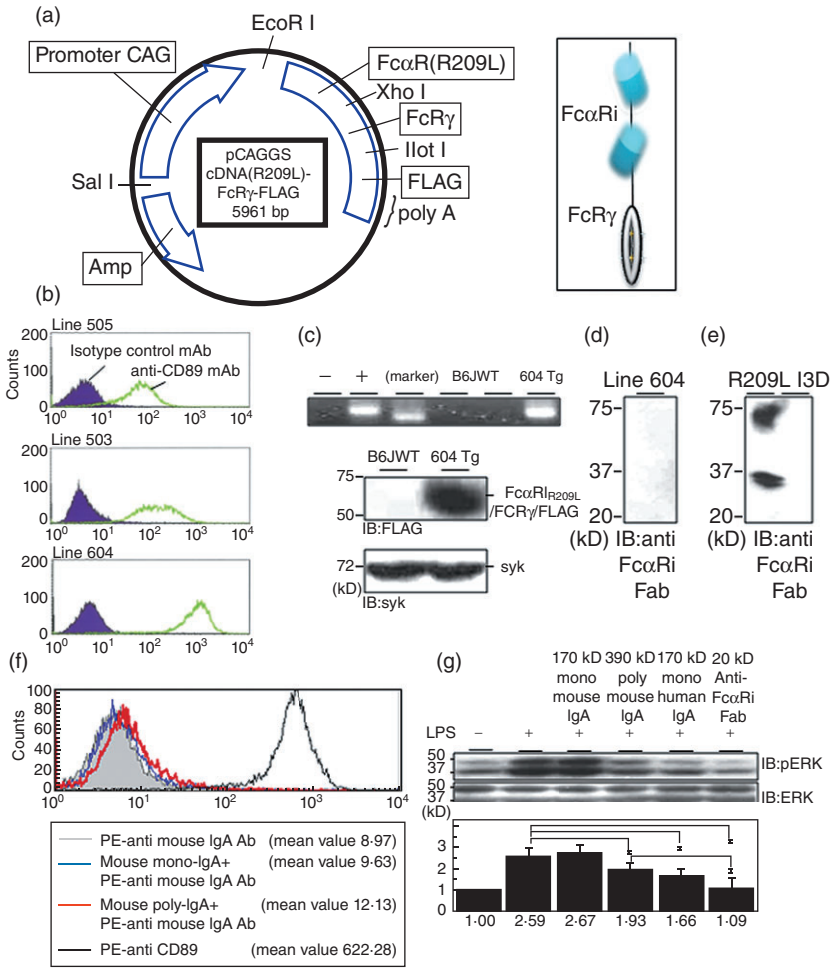

Fig. 1. Generation and characterization of FcαRI$_{R209L}$/FcRγ transgenic (Tg) mice. (a) Construct of the transgene consisting of the cDNA encoding human FcαRI$_{R209L}$/FcRγ-FLAG and the construct containing mouse β-actin promoter. Right figure shows simplified schematic of FcαRI$_{R209L}$/FcRγ. (b) Selected Tg mouse lines (503, 505 and 604), which expressed a large amount of human CD89 on cells. Cells were isolated from blood and stained with phycoerythrin (PE)-conjugated anti-CD89 monoclonal antibody (mAb) (open histograms) or PE-isotype control mAb (dark histograms). The level of transgene expression was highest on cells from line 604. (c) Genotyping and Western blot analysis. Genomic DNA was extracted from mouse tails [negative control, positive control, marker, C57BL/6J wild-type, littermate, Tg line 604 (from left to right)]. Lower figure shows an equal number of spleen cells from line 604 Tg or littermates by immunoblotting with anti-FLAG antibodies. Reprobing with anti-syk is shown as a control for equal loading. (d) FcαRI/FcRγ Tg did not produce soluble CD89. The blood cell lysate from line 604 was immunoprecipitated by anti-FcαRI antibodies coupled to beads, and immunoblotted with anti-FcαRI antibodies, but there was no CD89 band. This suggests that FcαRI adheres tightly to the FcRγ chain. (e) Mouse macrophage transfectant expressing a large amount of FcαRI/FcRγ (I3D cells) did not produce soluble CD89. Two kinds of cell supernatants (R209L transmembrane FcαRI mutants that could not associate with FcRγ or I3D cells) were collected. The supernatants were concentrated and immunoblotted with anti-FcαRI antibodies. However, the monomers (32 and 36 kD) and dimer (75 kD) of FcαRI bands were present in the left lane; there were no bands in the right lane. (f) Mouse immunoglobulin (Ig)A binding capacity to FcαRI on I3D cell surface. A representative experiment with flow cytometry analysis is shown. Mouse polymeric IgA was capable of weak binding with FcαRI, while mouse polymeric IgA plus soluble FcαRI were capable of strong binding. (g) Containment capacity of mouse monomeric IgA and human IgA preincubation in the Western blot experiment. Mouse monomeric IgA (170 kD) (100 μg/ml for 12 h), mouse polymeric IgA (>390 kD) (100 μg/ml), human IgA (170 kD) (100 μg/ml) and anti-FcαRI fragment antigen-binding (Fab) (10 μg/ml) were preincubated with I3D cells, which were then stimulated with lipopolysaccharide (LPS; Sigma Aldrich) (5 μg/ml for 3 min) and measured by immunoblotting with anti-phospho extracellular-regulated kinase (ERK) mitogen-activated protein kinase (MAPK) antibodies. Reprobing with anti-ERK is shown as a control for equal loading ($P < 0·05$).

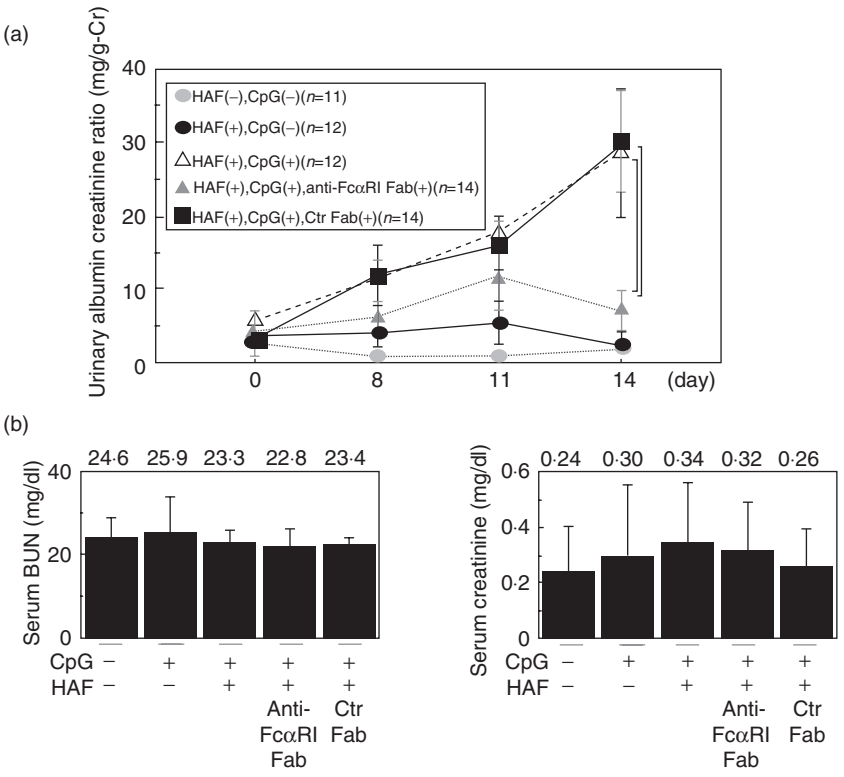

Fig. 2. Monovalent targeting of FcαRI decreases the amount of albuminuria but not the value of serum blood urea nitrogen (BUN) and creatinine levels after induction of horse apoferritin cytosine-guanine dinucleotide glomerulonephritis (HAF-CpG-GN). (a) Evaluation of morning albuminuria after injection of anti-FcαRI Fab and control Fab by enzyme-linked immunosorbent assay (ELISA) kit (Siemens). HAF-CpG-GN-induced albuminuria was measured when transgenic (Tg) mice were administered 10 μg/ml anti-FcαRI Fab but not administered with 10 μg/ml control Fab ($P < 0{\cdot}05$.). (b) Mouse BUN and creatinine levels were measured by Dri-Chem (Fujifilm Medical, Tokyo, Japan).

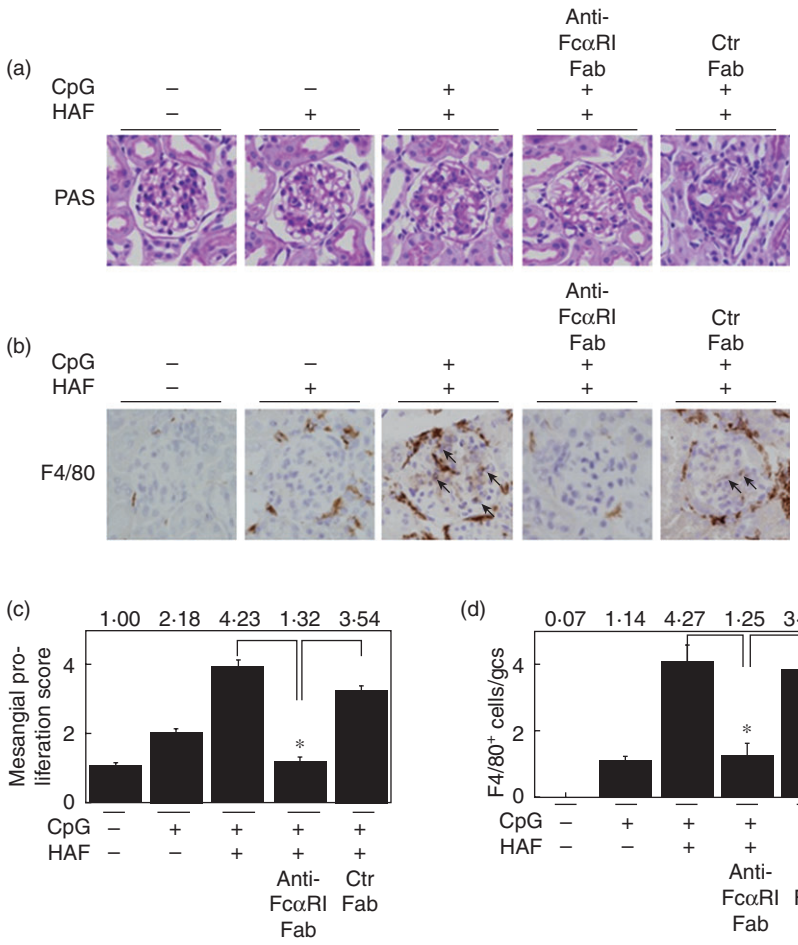

Fig. 3. Treatment with anti-FcαRI fragment antigen-binding (Fab) inhibits renal inflammation and macrophage infiltration in horse apoferritin cytosine-guanine dinucleotide glomerulonephritis (HAF-CpG-GN). Histological analysis [a, periodic acid-Schiff (PAS) staining] and immunohistological analysis (b, anti-mouse F4/80 antibody) of HAF-CpG-GN kidney sections from each group were performed on day 14. Corresponding quantitative evaluation of histological parameters by the disease severity score and number of infiltrating macrophages are shown (c,d). The glomerular lesions were evaluated using a semiquantitative scoring method, which was described previously ($P < 0{\cdot}05$).

FcαRI monomeric targeting blocks enhancement of renal cytokine and chemokine production stimulated by CpG-ODN treatment

To examine whether the increased number of glomerular macrophages in $FcαRI_{R209L}$/FcRγ mice was correlated with serum cytokine and chemokine levels, we performed ELISA assays with serum isolated from the affected mice. At day 14, treatment with CpG-ODN significantly increased excretion of TNF-α, RANTES and MCP-1, as described previously [19]. However, treatment with MIP8a Fab decreased TNF-α, RANTES and MCP-1 (Fig. 4a–c). These results indicated that MIP8a Fab inhibited harmful HAF-GN triggered by CpG-ODN at least in part by suppressing the Th1 immune response.

FcαRI targeting affects the humoral response to HAF

To examine the underlying mechanisms for treating disease by FcαRI targeting, we evaluated the effect of MIP8a Fab in the humoral immune response in mice with HAF-CpG-GN. Serum titers of total IgG were elevated to the same extent in the groups of HAF-injected mice (Fig. 5b), and the MIP8a Fab treatment group showed a small but not significantly decreased level of total IgG (Fig. 5b). However, serum IgG immune complexes purified with PEG were significantly higher in the PBS- or control Fab-treated group than in the MIP8a Fab-treated group in HAF-CpG-GN (Fig. 5c). The amounts of mesangial immune complex deposits assessed by immunofluorescence staining for IgG, IgG1, IgG2a and IgM and those of mesangial complement factor 3 deposits were also detected in HAF-injected groups (data not shown). Deposition of IgG2a and IgM in glomeruli was increased in the HAF-CpG-GN groups, as reported previously. Strikingly, deposition of not only IgM and IgG2a but also IgG1 and C3 disappeared completely after MIP8a Fab treatment (Fig. 5a and not shown). We also tried to measure inhibitory response using several antibodies which recognize FcαRI, including A59 Fab and human monomeric IgA, and confirmed that all these antibodies reduced the development of inflammation in HAF-CPG-GN (Fig. S1).

FcαRI monomeric targeting inhibits the expression of macrophage receptor 1 (MAC1), FcγRIIB and dendritic cell (DC)-specific intercellular adhesion molecule-3-grabbing non-integrin (DC-sIGn)

Cell-surface macrophage molecules including MAC1, FcγRIIB and DC-sIGn are implicated in presenting antigen to B cells. To determine whether anti-FcαRI targeting affect the expression of these molecules, I3D cells were treated with MIP8a Fab or control Fab. The cultured clone I3D spontaneously expresses high levels of MAC1, FcγRIIb and DC-sIGn when cultured in vitro (Fig. 6a–c). However, once these I3D cells were treated with MIP8a Fab for more than

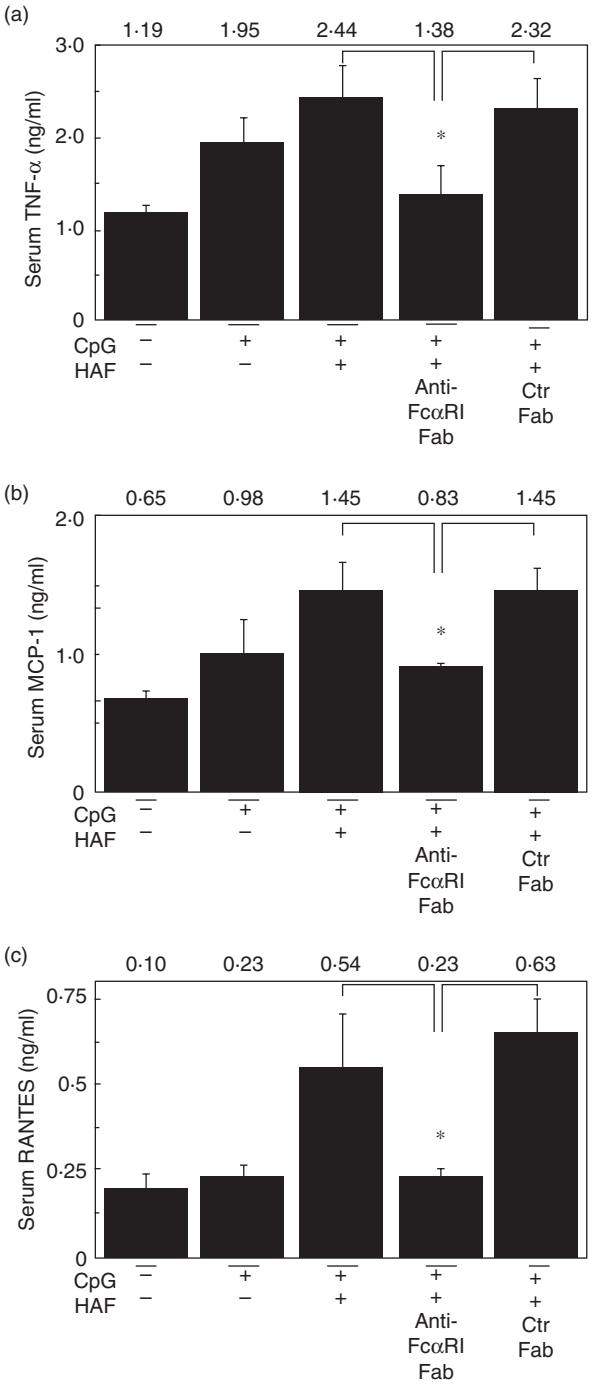

Fig. 4. Serum tumour necrosis factor (TNF)-α, monocyte chemoattractant protein-1 (MCP-1) and regulated upon activation normal T cell expressed and secreted (RANTES) production levels are decreased by anti-FcαRI fragment antigen-binding (Fab) treatment in horse apoferritin cytosine-guanine dinucleotide glomerulonephritis (HAF-CpG-GN). Serum TNF-α (a), MCP-1 (b) and RANTES (c) production in each HAF-CpG-GN group was measured by enzyme-linked immunosorbent assay (ELISA). Compared with the control Fab injection group, the anti-FcαRI Fab injection group showed lower protein production levels ($P < 0{\cdot}05$.).

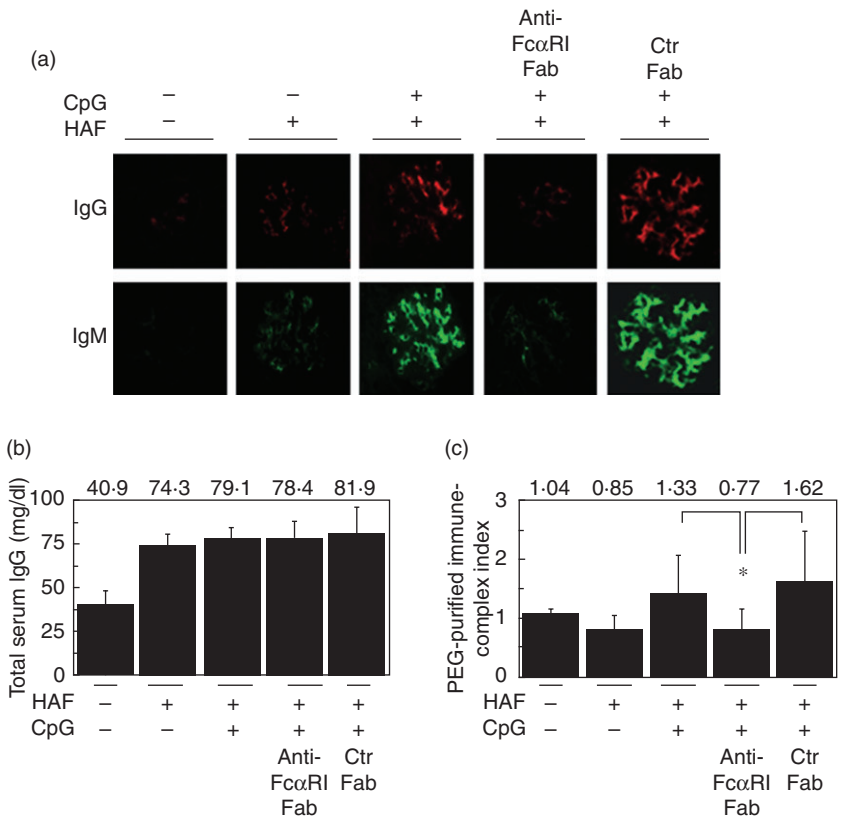

Fig. 5. Deposition of immunoglobulins (Ig) within glomeruli is eliminated completely by treatment with anti-FcαRI fragment antigen-binding (Fab) in a horse apoferritin cytosine-guanine dinucleotide (HAF-CpG) nephritis model. (a) Cryostat sections from each group were prepared, stained with phycoerythrin (PE) anti-mouse IgG or fluorescein isothiocyanate (FITC) anti-mouse IgM, and analysed by fluorescent microscopy (magnification ×100). (b) Serum total IgG levels were measured by enzyme-linked immunosorbent assay (ELISA). Data are expressed as mean ± standard deviation for a minimum of six mice in each group. There were no significant differences in the mean value of the corresponding control. (c) Detection of anti-HAF immunoglobulin in polyethylene glycol (PEG) precipitates from mice ($P < 0{\cdot}05$).

12 h, these expression levels of FcγRIIb and DC-sIGn but not MAC1 were decreased (Fig. 6a–c). The inhibitory effect of MIP8a Fab was concentration-dependent with maximal inhibition at a Fab concentration of 10 μg/ml (not shown). These data suggest that MIP8a Fab treatment of FcαRI on macrophages affects the expression of FcγRIIb and DC-sIGn.

Engraftment of FcαRI$_{R209L}$/FcRγ macrophages into wild-type (WT) mice is sufficient to decrease WT mice susceptibility to HAF-CpG-GN

After injection of FcαRI$_{R209L}$/FcRγ Tg macrophages into non-transgenic mice, all mice were injected with HAF prior to CpG. At day 14, mice treated with an unrelated control IgG developed elevated proteinuria, deposition of IgG and IgM, glomerular expansion and hypercellular changes and infiltration of CD11b^{+}/F4/80^{+} macrophage in glomeruli and interstitial tissue (Fig. 7a,b). However, all these signs of renal disease were attenuated significantly in mice treated with MIP8a Fab (Fig. 7a,b). These data suggest that MIP8a Fab treatment of FcαRI on macrophages is sufficient to protect against development of HAF-CpG-GN.

FcαRI monomeric targeting blocks CpG-induced activation of the ERK, p38 and JNK MAPKs pathways

We next analysed the effect of anti-FcαRI (MIP8a Fab) pre-treatment on TLR-9 signal transduction in response to CpG-ODN in the FcαR$_{R209L}$/FcRγ RAW 264·7 macrophage cell line (clone I3D). Key events in CpG-ODN-mediated signals, such as p38 and p42–p44 ERK MAPKs phosphorylation [20], are shown in Fig. 8a. However, these phosphorylations were inhibited strongly in I3D after preincubation with MIP8a Fab but not with control Fab (Fig. 8a). This inhibition was concentration- and time-dependent and showed the maximum effect after 12 h of preincubation (Fig. 8b,c). This treatment, although unlikely, does not kill the target cells (Fig. S2).

We also tested the effect of the physiological ligand IgA. Incubation with human monomeric IgA, but not IgG, resulted in an inhibitory response in I3D (Fig. 9).

Monovalent targeting of FcαRI$_{R209L}$/FcRγ functions as an inhibitor of TLR-9-induced transcriptional activation of NF-κB and AP-1

Figure 10 shows the effect of MIP8a Fab on CpG-ODN-induced transcriptional activation of the NF-κB/AP-1 cascade using a NF-κB/AP-1-Lux reporter construct. FcαRI/FcRγ transfected RAW 264·7 (I3D) cells transiently transfected with a NF-κB/AP-1-Lux reporter construct showed increased-NF-κB/AP-1 activity after CpG-ODN treatment. CpG DNA-activated NF-κB/AP-1-Lux was inhibited significantly after preincubation with MIP8a Fab but not with control Fab (Fig. 10). These results were dose- and time-dependent (data not shown). MIP8a Fab

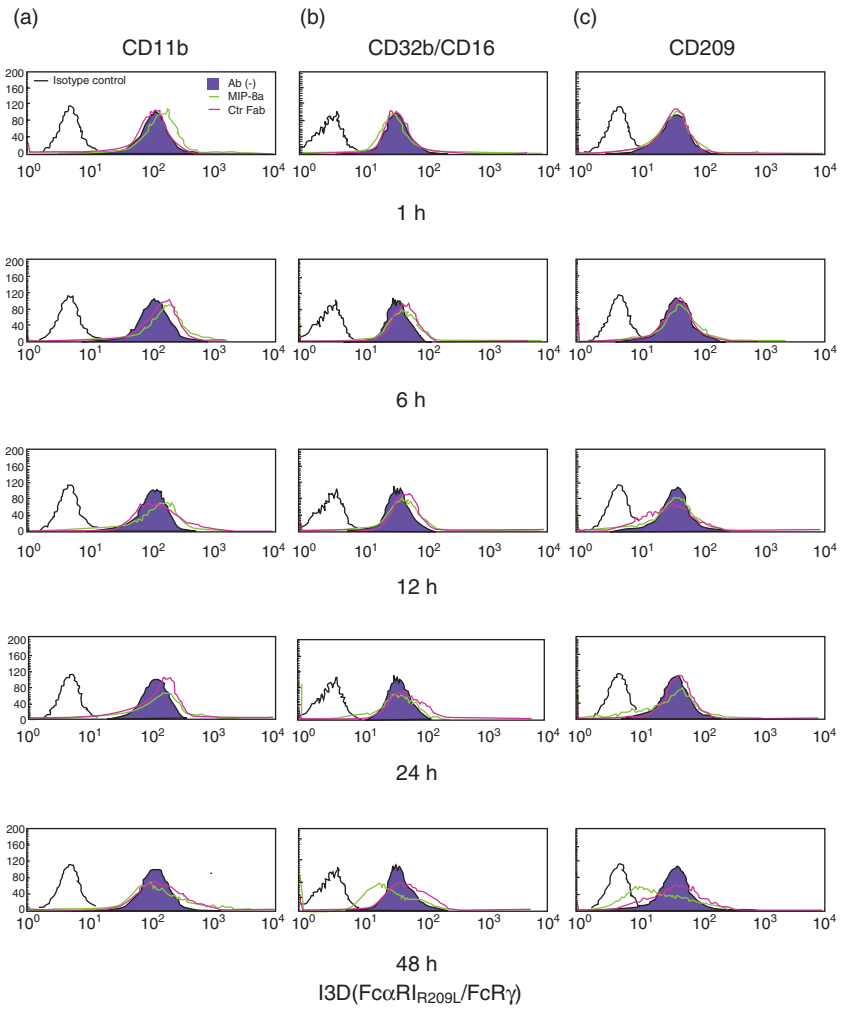

Fig. 6. Specific decreases in CD32b/CD16 and CD209 but not CD11b expression by anti-FcαRI targeting. CD11b (a), CD32b/CD16 (b) and CD209 (c) were stained with anti-mouse CD11b, CD32b/CD16 and CD209-phycoerythrin (PE), respectively (violet shaded histogram), comparatively with an irrelevant antibody (open white line) on I3D cells. I3D cells were subsequently preincubated at 37°C for 1, 6, 12, 24, 48 h, respectively, with anti-FcαRI fragment antigen-binding (Fab) (10 μg/ml) or control immunoglobulin (Ig)G Fab (10 μg/ml). The expression of CD11b, CD32b/CD16 and CD209 was then evaluated ($P < 0{\cdot}05$).

itself had no effect on basal NF-kB/AP-1-Lux activity (data not shown). Taken together, MIP8a Fab inhibits CpG-induced activation of the NF-κB/AP-1-Lux activity, providing a molecular basis for its inhibition of HAF-CpG-GN.

FcαRI monomeric targeting inhibits CpG-induced TNF-α/MCP-1 production in cultured FcαRI$_{R209L}$/FcRγ transfectants

I3D cells produced significantly greater amounts of TNF-α/MCP-1 after exposure to CpG (100 ng/ml) for 4 h (Fig. 11c), as described previously [19]. However, CpG-triggered TNF-α/MCP-1 production was inhibited significantly by pretreatment with MIP8a Fab but not control IgG (Fig. 11a). The inhibitory effect of MIP8a Fab was concentration-dependent with maximal inhibition at a Fab concentration of 10 μg/ml (Fig. 11b). MIP8a Fab at 10 μg/ml effectively inhibited CpG-induced TNF-α/MCP-1 production in I3D cells over a wide range of CpG concentrations (25–500 ng/ml).

Assessment of SHP-1 recruitment to FcαRI following CpG-ODN stimulation

The inhibitory activity of FcαRI has been linked with the recruitment of SH2-containing phosphatase SHP-1 [6]. To demonstrate this association further, we immunoprecipitated SHP-1 and found that FcRγ is co-immunoprecipitated in macrophages following treatment with MIP8a Fab, and this association was dependent on anti-FcαRI Fab, but not CpG-ODN, stimulation (Fig. 12a). No association between SHP-1 and FcRγ was found after multivalent cross-linking of FcαRI (data not shown), confirming data described previously for FcαRI pull-downs [16]. Therefore, we directly tested the role of SHP-1 activity in CpG-ODN-stimulated peripheral macrophages supporting SHP-1 involvement in ITAM-mediated inhibition of different receptor systems. As shown in Fig. 12b, MIP8a Fab pretreatment strongly induced activation of SHP-1 measured by Sensolyte pNPP protein phosphatase assay kit. These results support SHP-1 involvement in ITAM-mediated inhibition of the TLR-9 signalling systems.

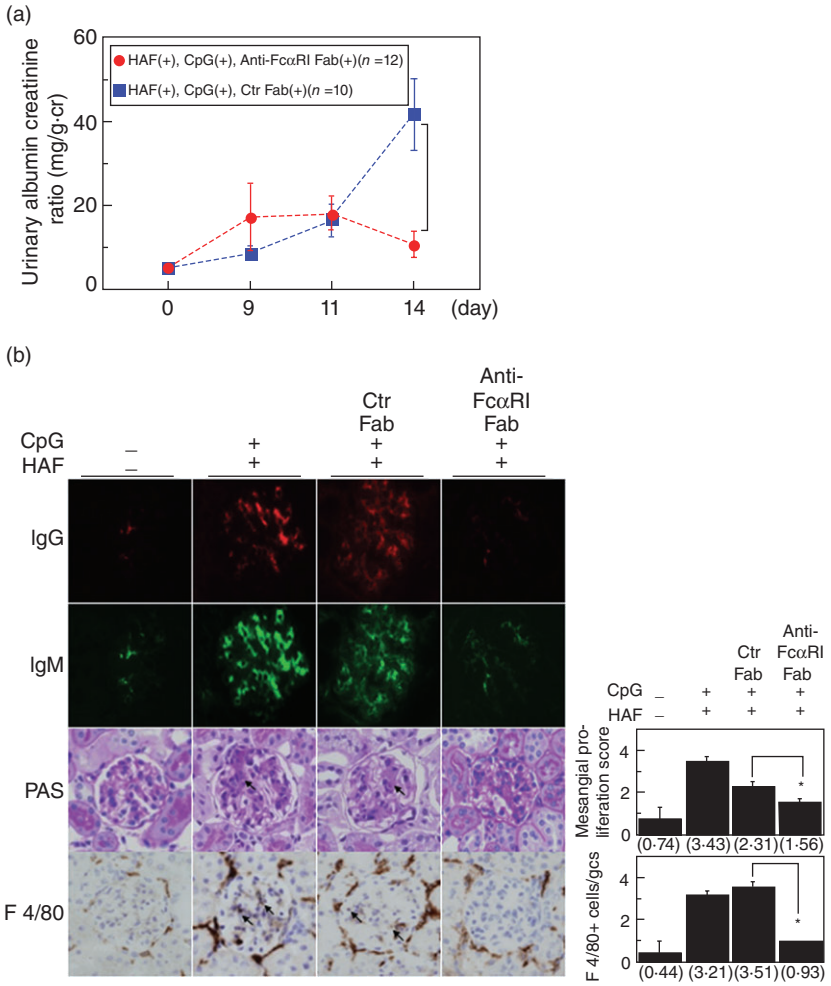

Fig. 7. Adoptive transfer of FcαRI$_{R209L}$/FcRγ macrophages reduces development of horse apoferritin cytosine-guanine dinucleotide glomerulonephritis (HAF-CpG-GN) in wild-type (WT) mice. Macrophages (2x10^6) obtained from FcαRI$_{R209L}$/FcRγ transgenic (Tg) spleen were injected into the lateral tail vein of C57BL/6J before injection of anti-FcαRI fragment antigen-binding (Fab)or control Fab. (a) Morning albuminuria from each group was measured by an enzyme-linked immunosorbent assay (ELISA) kit (Siemens). Significant difference from the mean value of the corresponding control. (b) Appearance of mesangial immunoglobulin (Ig)G or IgM deposits, periodic acid-Schiff (PAS) staining and CD11b-positive cells from C57BL/6J on day 14 in the HAF-CpG-GN were analysed ($P < 0{\cdot}05$).

Discussion

We have demonstrated recently that inhibitory signalling by myeloid FcαRI, in addition to its proinflammatory function, could trigger a powerful anti-inflammatory effect [6,16]. In the present study, we investigated the hypothesis that inhibitory signals via FcαRI could block TLR-9 signal transduction that was thought to be a key player in the development of renal inflammation. To address these issues, we used an HAF-CpG-GN experimental model that could aggravate HAF immune complex glomerulonephrits via the enhanced TLR-9 signalling pathway. We showed that FcαRI$_{R209L}$/FcRγ Tg mice treated with anti-FcαRI Fab have decreased susceptibility to HAF-CpG-GN via the TLR-9 signalling pathway. Adoptive transfer experiments confirmed a critical role for FcαRI in the negative regulation of macrophage function in HAF-CpG-GN. Taken together, our data demonstrate that monovalent targeting of FcαRI mediates a decreased influx of macrophages, thereby improving renal function in CpG-ODNs models of renal disease.

Because potent inhibitory ITAM (iITAM) signalling triggered by monovalent targeting of FcαRI requires an associated FcRγ chain [6], we generated a novel transgenic mouse expressing the FcαRI$_{R209L}$/FcRγ chimeric receptor (FcαRI$_{R209L}$/FcRγ Tg). Unexpectedly, this Tg mouse did not show any signs of inflammation in a spontaneous course of at least 12 months (data not shown), whereas FcαRI Tg mice spontaneously developed massive mesangial IgA deposition, glomerular and interstitial macrophage infiltration, mesangial matrix expansion, haematuria and mild proteinuria [14,19]. The molecular mechanism was shown to involve soluble FcαRI released after interaction with IgA, and this release was independent of the FcαRI association with the FcRγ chain [21]. In the present study, we demonstrated that mouse IgA did not induce shedding of FcαRI from macrophage transfectants expressing FcαRI$_{R209L}$ associated with FcRγ (I3D) (Fig. 1e). However, a mutated receptor could not be associated with the FcRγ induced shedding of soluble FcαRI (Fig. 1e). This led us to the conclusion that soluble FcαRI release depends on the interaction with IgA and FcαRI which is not associated with the γ chain (γ less FcαRI). Indeed, we did not find soluble FcαRI in the serum of FcαRI$_{R209L}$/FcRγ Tg mice (Fig. 1d). The results in WT FcαRI Tg mice demonstrated that expression of FcαRI on

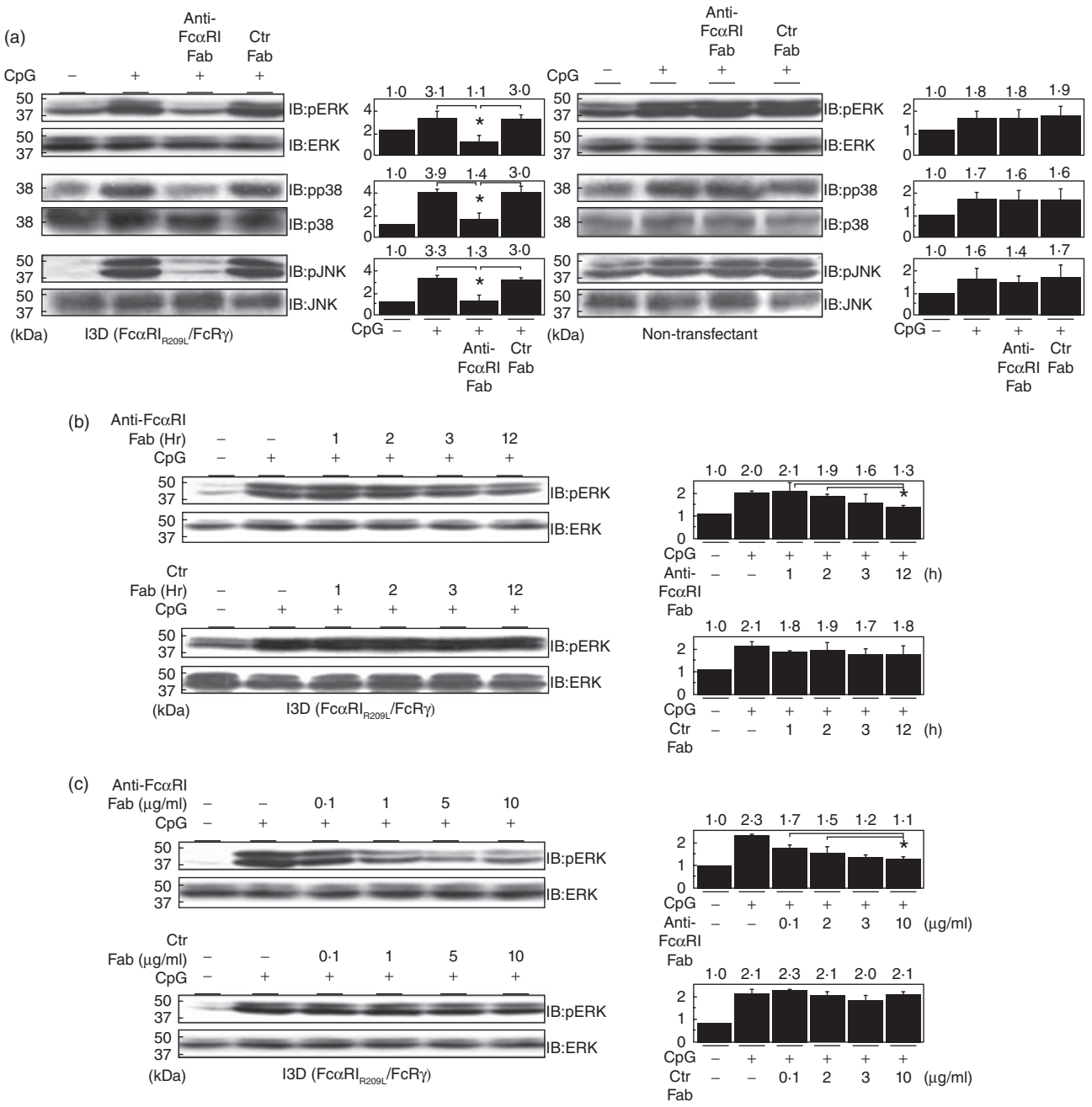

Fig. 8. Cytosine-guanine dinucleotide (CpG)-mediated mitogen-activated protein kinase (MAPK) signalling in FcαRI$_{R209L}$/FcRγ mouse macrophage transfectants is inhibited by anti-FcαRI fragment antigen-binding (Fab) treatment. (a) MAPKs [extracellular-regulated kinase (ERK), p38 and c-Jun N-terminal kinase (JNK)] phosphorylation reactions in FcαRI$_{R209L}$/FcRγ mouse macrophage transfectant (clone I3D) and untreated RAW264·7 macrophages before and after CpG stimulation (5 μg/ml for 10 min) were measured by immunoblotting with phospho-specific antibodies. Reprobing with anti-ERK, p38 and JNK was used as control for equal loading. CpG-mediated MAPKs (ERK, p38 and JNK) phosphorylation reactions were inhibited when cells were preincubated with anti-FcαRI Fab (10 μg/ml for 12 h) but not after preincubation with control Fab (10 μg/ml for 12 h). Kinetics (b) and dose–response (c) of the effect of anti-FcαRI Fab *versus* control Fab are shown. All transfection experiments were performed at least in triplicate ($P < 0·05$).

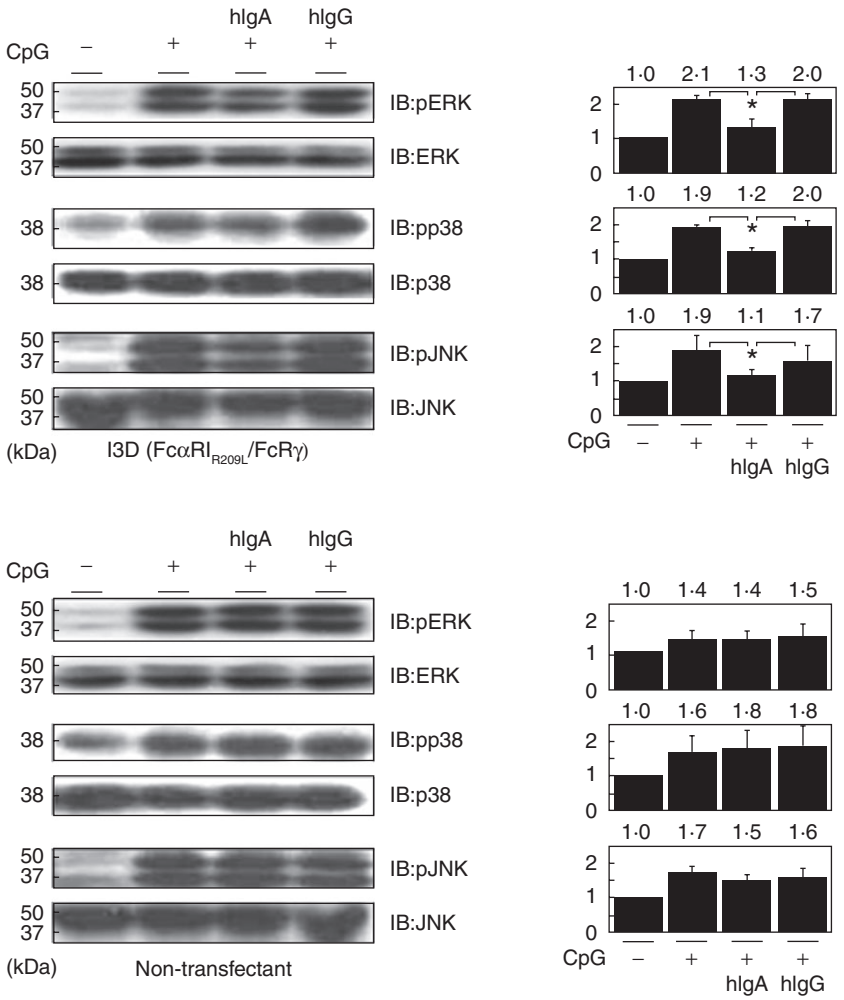

Fig. 9. Human serum immunoglobulin (Ig)A blocks mitogen-activated protein kinase (MAPK) phosphorylation induced by cytosine-guanine dinucleotide (CpG) in mouse macrophage transfectant (clone I3D). I3D and untreated RAW264·7 (non-transfectant) cells were stimulated with CpG (5 μg/ml for 10 min) after preincubation with human IgA or human IgG (100 μg/ml for 12 h). MAPK [extracellular-regulated kinase (ERK), p38, c-Jun N-terminal kinase (JNK)] phosphorylation reaction was measured by immunoblotting with phospho-specific antibodies. Reprobing with anti-ERK, p38 and JNK are shown as controls for equal loading. The results were from three independent experiments ($P < 0{\cdot}05$).

mouse monocytes/macrophages was detrimental [21]. The mechanism underlying spontaneous IgA nephropathy (IgAN) onset in WT FcαRI Tg mice is probably linked to mouse serum IgA, which is predominantly polymeric (70–80% of total serum IgA), contrary to the situation in humans [21]. We next analysed the ability of FcαRI$_{R209L}$/FcRγ to bind to human and mouse IgA. No specific binding of mouse monomeric IgA was observed, whereas binding of mouse polymeric IgA (>390 kD) from line 604 to FcαRI was significant (Fig. 1f). These experiments indicated that FcαRI could bind polymeric but not mouse monomeric IgA. We then found that polymeric mouse IgA which could bind weakly to FcαRI$_{R209L}$/FcRγ transfectants was sufficient to induce strong inhibitory signals and blocked TLR-4 signal triggered by LPS (Fig. 1g). These findings suggested that the association of FcαRI and FcRγ blocks the shedding of FcαRI, and weak phosphorylation of iITAM by low-affinity mouse polymeric IgA is protective against cell activation and prevents IgAN development.

In the present study, we observed that monovalent targeting of FcαRI was inhibitory in an *in vivo* model of TLR-9 signalling-accelerated nephritis, showing a possible explanation of inhibitory mechanisms. First, TLR-9 and probably proinflammatory cytokines including MCP-1 and TNF-α are thought to activate macrophage MAPKs (p38, ERK1/2 and JNK) and NF-κB/AP-1 pathways, promoting gene expression and cytokine production (MCP-1, RANTES and MIP-1a) [21,22], leading to cytokine-mediated inflammation and nephritis [23]. Consistent with this, the present study showed that both MAPKs (p38, JNK and ERK1/2) and NF-κB/AP-1 are activated significantly in the inflamed kidneys enhanced by TLR-9 activation via CpG-ODN (not shown). Our observation (Figs 2–4) that TLR-9 orchestrates the production of an array of potential mediators of renal injury makes it an attractive target for the prevention or treatment of acute renal injury. Indeed, pharmacological blockade of MAPKs activation, specifically ERK and p38, improved disease activity and the histological disease score in experimental kidney diseases [24]. Our mechanistic analysis revealed that monovalent targeting of FcαRI regulates CpG-ODN-induced activation of MAPKs, primarily ERK1/2, p38, JNK and NF-κB/AP-1 activation via TLR-9, leading to down-regulation of TNF-α and MCP-1 (Figs 8–11). These data suggest that abolished activation of p38,

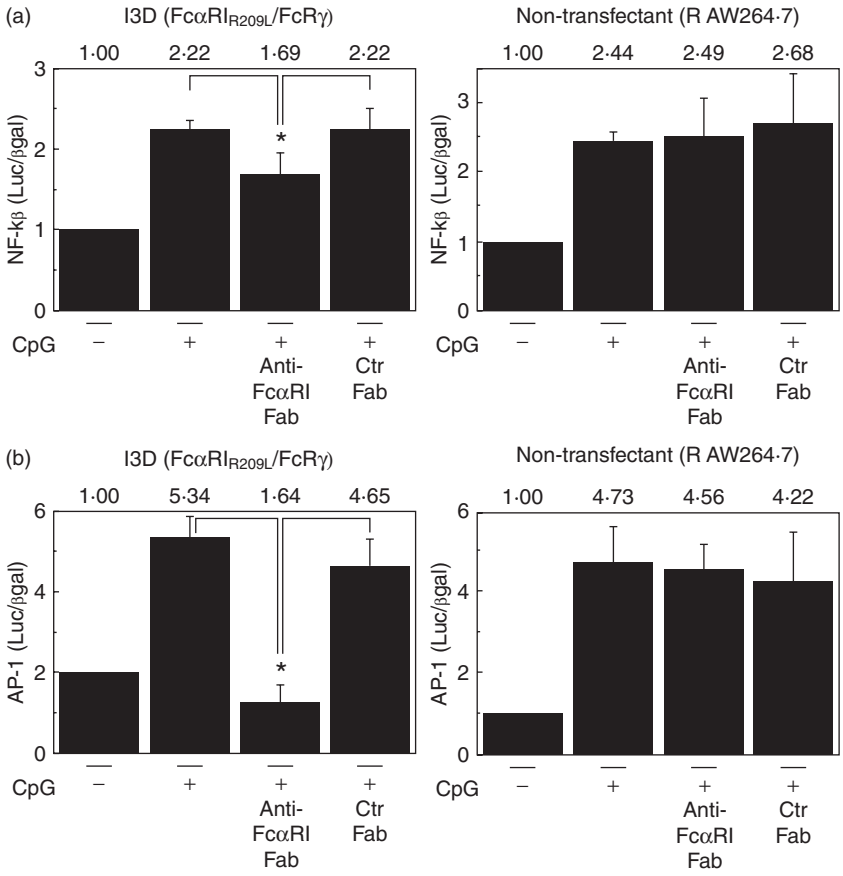

Fig. 10. Monovalent targeting using anti-FcαRI fragment antigen-binding (Fab) attenuates macrophage transcriptional activities of nuclear factor (NF)-κB/AP-1 induced by Toll-like receptor-9 (TLR-9) signalling with CpG-oligodeoxynucleotide (ODN). I3D and untreated RAW264·7 cells (1×10^5 /ml) were cultured, and plasmid DNA (NF-κB-Lux, AP-1-Lux) was assessed as described in Materials and methods. CpG stimulation was performed for 10 min after preincubation with anti-FcαRI fragment antigen-binding (Fab) or control Fab. NF-κB (a) and activator protein (AP)-1 (b) activities were determined. All transfection experiments were performed at least in triplicate ($P < 0{\cdot}05$).

ERK1/2 and JNK via TLR-9 stimulation through FcαRI targeting in the FcαRI$_{R209L}$/FcRγ Tg is sufficient to regulate increased cell activation and control of HAF-CpG-GN. Secondly, recent findings in both human and mouse models suggest that TLR-9 may play a central role in maintenance and progression of systemic lupus erythematosus (SLE) by promoting elevated IFN-α levels from human plasmacytoid dendritic cells (PDC) and by activating B cells to produce autoantibodies [25]. Studies from the Hartmann laboratory [26] first suggested that chromatin or ssRNA components of SLE immunocomplexes can activate TLR-9 in intracellular endosomes of B cells. Such nucleic acid-containing immunocomplexes were shown to activate autoreactive B cells and autoantibody production. TLR-9-active sequence transgenic mice produce large amounts of anti-RNA, -DNA and -nucleosome antibodies of the IgG2a and IgG2b isotype that cause nephritis [27]. B cells can promptly detect and mount responses to antigen after immunization. In the case of small soluble antigens, responses can be mounted following a simple diffusion of antigen into the lymphoid tissue; however, these encounters are usually mediated through macrophages, DCs and follicular DCs. In addition, macrophages are known to express a wide range of cell-surface receptors that could participate in the presentation of unprocessed antigen, including complement receptors, pattern recognition receptors and/or carbohydrate-binding scavenger receptors [28]. Indeed, macrophage receptor 1 (MAC1; also known as αMβ2 integrin and CD11b–CD18 dimer), which is a receptor for complement component 3 (C3) that is expressed by macrophages, has been suggested to contribute to the retention of antigen on the cell surface [29]. Alternatively, the inhibitory low-affinity receptor for IgG (FcγRIIB) might mediate the internalization and recycling of IgG-containing immune complexes to the macrophage cell surface, as has been shown in DCs [30]. Finally, the C-type lectin DC-specific ICAM3-grabbing non-integrin (DC-sIGn; also known as CD209) could participate in the retention of glycosylated antigens, which is consistent with the observation that mice deficient in the mouse homologue of DC-sIGn, sIGnR1, fail to mount humoral immune responses following infection with *Streptococcus pneumonia* [31]. The cultured clone I3D spontaneously expresses a high level of MAC1, FcγRIIb and DC-sIGn when cultured *in vitro* (Fig. 6). However, once these I3D cells were treated with MIP8a Fab more than 12 h, these expression levels of FcγRIIb and DC-sIGn but not MAC1 were decreased. The inhibitory effect of MIP8a Fab was concentration-dependent, with maximal inhibition at a Fab concentration of 10 μg/ml (Fig. 6). We believe these results could be one of the mechanisms that explain why MIP8a Fab treatment inhibits antibody deposition and subsequent complement activation.

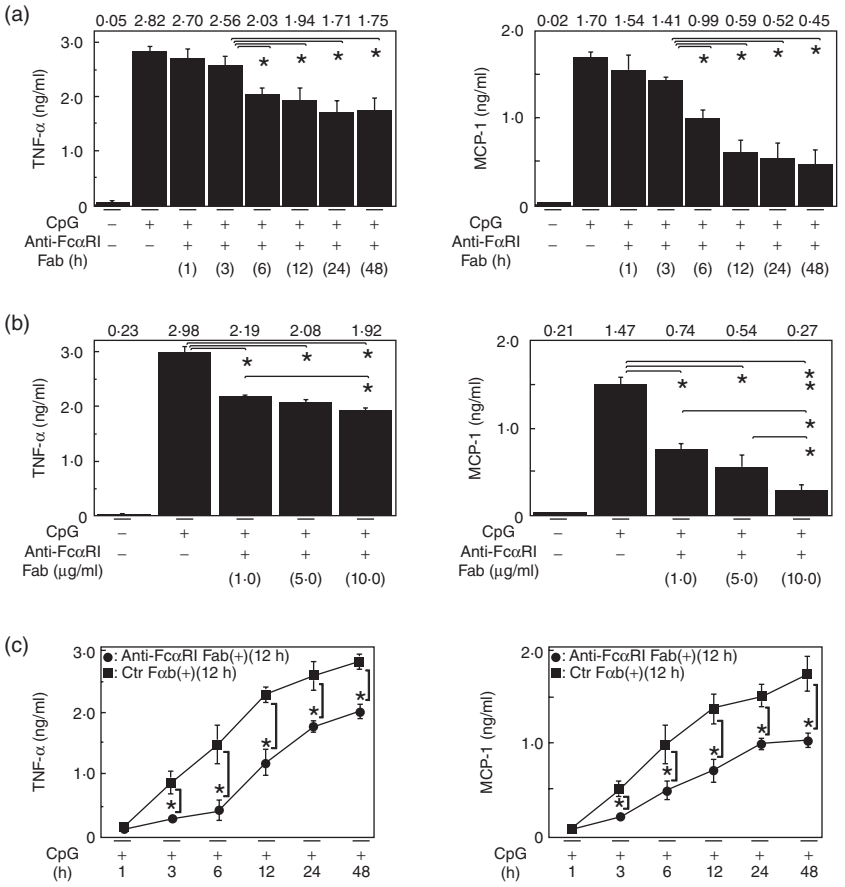

Fig. 11. Treatment with anti FcαRI fragment antigen-binding (Fab) inhibits cytosine-guanine dinucleotide (CpG)-induced tumour necrosis factor (TNF)-α and monocyte chemoattractant protein-1 (MCP-1) production in an *in vitro* study with $FcαRI_{R209L}$/FcRγ mouse macrophage transfectants. TNF-α and MCP-1 production levels were measured by enzyme-linked immunosorbent assay (ELISA) after stimulation with CpG. Kinetics (a) and dose–response (b) of the effect of anti-FcαRI Fab on CpG-induced (100 ng/ml, 4 h) TNF-α and MCP-1 production levels by I3D cells. (a) I3D cells were treated with anti-FcαRI Fab (10 μg/ml) for the indicated time (0, 1, 3, 6, 12, 24 or 48 h) and exposure to CpG. (b) I3D cells were treated with anti-FcαRI Fab (12 h) for the indicated concentration (0, 1, 5, 10 μg/dl) and stimulated with CpG. The results were from three independent experiments ($P < 0·05$). (c) Cultured I3D cells in 96-well plates (2×10^5 cells/well at 37°C) were stimulated with CpG (100 ng/ml) for the indicated time after preincubation with anti-FcαRI Fab or control Fab (each 10 μg/ml, 12 h). CpG-mediated TNF-α /MCP-1 production levels were measured by ELISA. The results were from three independent experiments ($P < 0·05$).

Taken together, these data suggest that the role of TLR-9 signalling in macrophages is predominant in the progression of HAF-CpG-GN and blockade of this signalling by monovalent targeting of FcαRI might inhibit disease activity.

The inhibitory activity of $FcαRI_{R209L}$/FcRγ ITAM (iITAM) has been associated with SHP-1 recruitment following weak activation [6,32]. We demonstrated that stimulation of macrophages with CpG-ODN after MIP8a Fab pretreatment induced weak tyrosine phosphorylation of $FcαRI_{R209L}$/FcRγ ITAM and recruitment of phosphatase SHP-1 but not SHP-2. These findings indicate clearly that iITAM is activated on ligation with CpG-ODN, and suggest that SHP-1 may be involved in the negative regulation of ERK1/2 and p38 by TLR-9. SHP-1 can negatively regulate MAPKs (ERK and JNK) activation directly and indirectly [33,34]. Nitric oxide-induced dephosphorylation of ERK1/2 in rat vascular smooth muscle cells was associated with SHP-1 interaction and activation. Notably, ERK1/2 dephosphorylation was attenuated by SHP-1 inhibitor. Furthermore, SHP-1 dephosphorylates vascular endothelial growth factor (VEGF)-induced ERK phosphorylation in endothelial cells [35]. In contrast to iITAM, SIRP-1a, ITIM-bearing receptor, inhibits lipopolysaccharide/TLR-4-mediated signalling primarily through sequestering SHP-2 but not SHP-1 [36], suggesting that different inhibitory receptors may utilize divergent intracellular phosphatases to elicit their inhibitory effects.

In conclusion, our data suggest that the deterioration of HAF-GN triggered by CpG-ODN was suppressed dramatically by monovalent targeting of FcαRI. As TLR-9 signalling in macrophages is thought to be one of the major inflammatory molecular mechanisms, our data establish the strong anti-inflammatory potential of FcαRI after monovalent targeting of microbial infection stimuli. Given its expression pattern, we propose that FcαRI-targeted therapeutic strategies may prove to be particularly useful for inflammatory diseases with major involvement of myeloid cells.

Acknowledgements

We thank N. Nakano PhD (Juntendo University Atopy Research Center) for technical supports and E. Nakamura (Research Institute for Diseases of Old Age, Juntendo University Faculty of Medicine) with animal care. This work was supported by Grants from Takeda Science Foundation and Japan Research Foundation for Clinical Pharmacology.

Disclosure

All authors declare that they have no conflicts of interest.

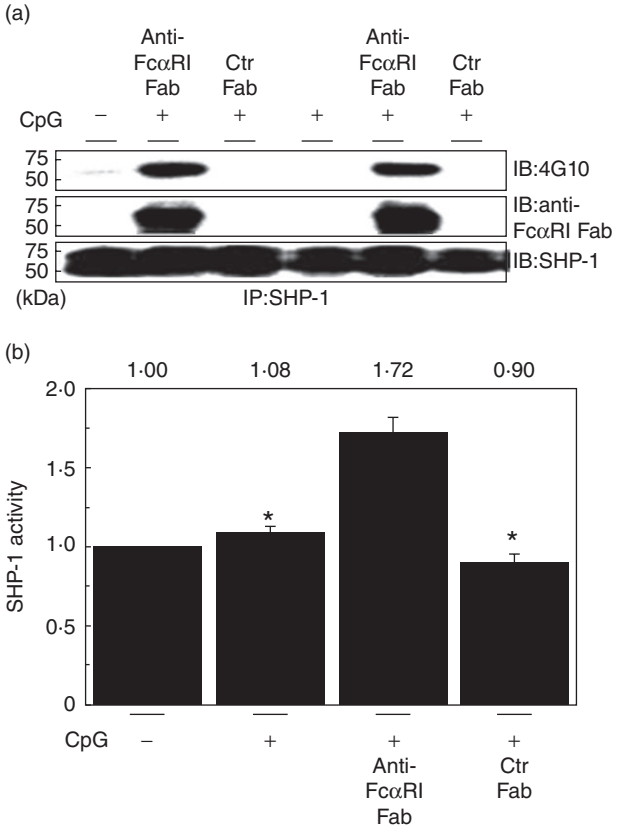

Fig. 12. Src homology phosphatase 1 (SHP1) phosphorylation is the key role of the FcαRI blockade mechanism. (a) Cytosine-guanine dinucleotide (CpG) (5 μg/ml for 10 min) was added to I3D after preincubation with anti-FcαRI fragment antigen-binding (Fab) or control Fab (10 μg/ml for 12 h). The samples were purified by an immunoprecipitation assay with anti-SHP1 immunoglobulin (Ig)G and assayed by immunoblotting with 4G10 anti-phosphotyrosine (PY) or anti-FcαRI Fab. Blots were stripped and reprobed with anti-SHP1 to judge effective immunoprecipitation. (b) Using the immunoprecipitated samples, activity of SHP1 was measured by Sensolyte pNPP protein phosphatase assay kit. The rate of formation of *p*NPP was determined by spectrophotometry at 405 nm. Experiments were repeated three times ($P < 0{\cdot}05$).

References

1 Van Parijs L, Abbas AK. Homeostasis and self-tolerance in the immune system: turning lymphocytes off. Science 1998; **280**:243–8.

2 Ravetch JV, Lanier LL. Immune inhibitory receptors. Science 2000; **290**:84–9.

3 Burshtyn DN, Lam AS, Weston M, Gupta N, Warmerdam PA, Long EO. Conserved residues amino-terminal of cytoplasmic tyrosines contribute to the SHP-1-mediated inhibitory function of killer cell Ig-like receptors. J Immunol 1997; **162**:897–902.

4 Pfefferkorn LC, Yeaman GR. Association of IgA-Fc receptors (Fc alpha R) with Fc epsilon RI gamma 2 subunits in U937 cells. Aggregation induces the tyrosine phosphorylation of gamma 2. J Immunol 1994; **153**:3228–36.

5 Launay P, Patry C, Lehuen A, Pasquier B, Blank U, Monteiro RC. Alternative endocytic pathway for immunoglobulin A Fc receptors (CD89) depends on the lack of FcRgamma association and protects against degradation of bound ligand. J Biol Chem 1999; **274**:7216–25.

6 Pasquier B, Launay P, Kanamaru Y *et al.* Identification of FcalphaRI as an inhibitory receptor that controls inflammation: dual role of FcRgamma ITAM. Immunity 2005; **22**:31–42.

7 Hamerman JA, Jarjoura JR, Humphrey MB, Nakamura MC, Seaman WE, Lanier LL. Cutting edge: inhibition of TLR and FcR responses in macrophages by triggering receptor expressed on myeloid cells (TREM)-2 and DAP12. J Immunol 2006; **177**:2051–5.

8 Wang L, Gordon RA, Huynh L *et al.* Indirect inhibition of Toll-like receptor and type I interferon responses by ITAM-coupled receptors and integrins. Immunity 2010; **32**:518–30.

9 Kobayashi K, Hernandez LZ, Galan JE, Janeway Jr CA, Medzhitov R, Flavell RA. IRAK-M is a negative regulator of Toll-like receptor signaling. Cell 2002; **110**:191–202.

10 Takeda K, Kaisho T, Akira S. Toll-like receptors. Annu Rev Immunol 2003; **21**:335–76.

11 Hemmi H, Takeuchi O, Kawai T *et al.* A Toll-like receptor recognizes bacterial DNA. Nature 2000; **408**:740–5.

12 Krieg AM. CpG motifs in bacterial DNA and their immune effects. Annu Rev Immunol 2002; **20**:709–60.

13 Yeo SJ, Yoon JG, Yi AK. Myeloid differentiation factor 88-dependent post-transcriptional regulation of cyclooxygenase-2 expression by CpG DNA: tumor necrosis factor-alpha receptor-associated factor 6, a diverging point in the Toll-like receptor 9-signaling. J Biol Chem 2003; **278**:40590–600.

14 Iskandar SS, Jennette JC. Influence of antibody avidity on glomerular immune complex localization. Am J Pathol 1983; **112**:155–9.

15 Anders HJ, Frink M, Linde Y *et al.* CC chemokine ligand 5/RANTES chemokine antagonists aggravate glomerulonephritis despite reduction of glomerular leukocyte infiltration. J Immunol 2003; **170**:5658–66.

16 Kanamaru Y, Pfirsch S, Aloulou M *et al.* Inhibitory ITAM signaling by Fc alpha RI-FcR gamma chain controls multiple activating responses and prevents renal inflammation. J Immunol 2008; **180**:2669–78.

17 Raij L, Azar S, Keane W. Mesangial immune injury, hypertension, and progressive glomerular damage in Dahl rats. Kidney Int 1984; **26**:137–43.

18 Sato M, Watanabe T, Oshida A, Nagashima A, Miyazaki JI, Kimura M. Usefulness of double gene construct for rapid identification of transgenic mice exhibiting tissue-specific gene expression. Mol Reprod Dev 2001; **60**:446–56.

19 Anders HJ, Banas B, Linde Y *et al.* Bacterial CpG-DNA aggravates immune complex glomerulonephritis: role of TLR9-mediated expression of chemokines and chemokine receptors. J Am Soc Nephrol 2003; **14**:317–26.

20 Ravindran C, Cheng YC, Liang SM. CpG-ODNs induces up-regulated expression of chemokine CCL9 in mouse macrophages and microglia. Cell Immunol 2010; **260**:113–18.

21 Launay P, Grossetete B, Arcos-Fajardo M *et al.* Fcalpha receptor (CD89) mediates the development of immunoglobulin A (IgA) nephropathy (Berger's disease). Evidence for pathogenic soluble receptor-Iga complexes in patients and CD89 transgenic mice. J Exp Med 2000; **191**:1999–2009.

22 Kazimierczak K, Kopec W, Klinger M. Toll-like receptors (TLR) in the pathogenesis of kidney diseases. Pol Merkur Lekarski 2007; **23**:382–5.

23 Ho AW, Wong CK, Lam CW. Tumor necrosis factor-alpha up-regulates the expression of CCL2 and adhesion molecules of human proximal tubular epithelial cells through MAPK signaling pathways. Immunobiology 2008; **213**:533–44.
24 Stambe C, Atkins RC, Tesch GH *et al.* Blockade of p38alpha MAPK ameliorates acute inflammatory renal injury in rat anti-GBM glomerulonephritis. J Am Soc Nephrol 2003; **14**:33851.
25 Wu P, Wu J, Liu S *et al.* TLR9/TLR7-triggered downregulation of BDCA2 expression on human plasmacytoid dendritic cells from healthy individuals and lupus patients. Clin Immunol 2008; **129**:40–8.
26 Hornung V, Schlender J, Guenthner-Biller M *et al.* Replication-dependent potent IFN-alpha induction in human plasmacytoid dendritic cells by a single-stranded RNA virus. J Immunol 2004; **173**:5935–43.
27 Giordani L, Sanchez M, Libri I, Quaranta MG, Mattioli B, Viora M. IFN-alpha amplifies human naive B cell TLR-9-mediated activation and Ig production. J Leukoc Biol 2009; **86**:261–71.
28 Taylor PR, Martinez-Pomares L, Stacey M, Lin HH, Brown GD, Gordon S. Macrophage receptors and immune recognition. Annu Rev Immunol 2005; **23**:901–44.
29 Phan T, Grigorova I, Okada T, Cyster J. Subcapsular encounter and complement-dependent transport of immune complexes by lymph node B cells. Nat Immunol 2007; **8**:992–1000.
30 Bergtold A, Desai DD, Gavhane A, Clynes R. Cell surface recycling of internalized antigen permits dendritic cell priming of B cells. Immunity 2005; **23**:503–14.
31 Koppel EA, Wieland CW, van den Berg VC *et al.* Specific ICAM-3 grabbing nonintegrin-related 1 (SIGNR1) expressed by marginal zone macrophages is essential for defense against pulmonary *Streptococcus pneumoniae* infection. Eur J Immunol 2005; **35**:2962–9.
32 Kanamaru Y, Tamouza H, Pfirsch S *et al.* IgA Fc receptor I signals apoptosis through the FcRgamma ITAM and affects tumor growth. Blood 2007; **109**:203–11.
33 Bartoe JL, Nathanson NM. Differential regulation of leukemia inhibitory factor-stimulated neuronal gene expression by protein phosphatases SHP-1 and SHP-2 through mitogen-activated protein kinase-dependent and -independent pathways. J Neurochem 2000; **74**:202132.
34 Lee K, Esselman WJ. Inhibition of PTPs by H(2)O(2) regulates the activation of distinct MAPK pathways. Free Radic Biol Med 2002; **33**:1121–32.
35 Song M, Park JE, Park SG *et al.* NSC-87877, inhibitor of SHP-1/2 PTPs, inhibits dual-specificity phosphatase 26 (DUSP26). Biochem Biophys Res Commun 2009; **381**:491–5.
36 Smith RE, Patel V, Seatter SD *et al.* A novel MyD-1 (SIRP-1alpha) signaling pathway that inhibits LPS-induced TNFalpha production by monocytes. Blood 2003; **102**:2532–40.

Supporting information

Additional supporting information may be found in the online version of this article.

Fig. S1. Targeting of anti-FcαRI with mouse monoclonal 8a (MIP8a) treatment eliminates mouse glomerular deposition of immunoglobulins in horse apoferritin cytosine-guanine dinucleotide (HAF-CpG) nephritis compared to the other Fc receptor targetings. In each group, HAF was administered once daily as above. At days 7 and 8, 20 μg of each antibody [MIP-8a, A59, human monomeric immunoglobulin A (mIg)A, control fragment antigen-binding (Fab)] in 200 μl of saline was administered via the caudal vein after 40 μg of endotoxin-free CpG-oligodeoxynucleotides (ODN) administered intraperitoneally. At day 14, renal tissues were collected and cryostat sections were stained with fluorescein isothiocyanate (FITC) anti-mouse IgM, and analysed by fluorescent microscopy (magnification × 100).

Fig. S2. FcαRI targeting do not kill the target cells in $Fc\alpha RI_{R209L}$/FcRγ transgenic (Tg) mouse and $Fc\alpha RI_{R209L}$/FcRγ mouse macrophage transfectants (I3D) by use of mouse monoclonal 8a (MIP8a) fragment antigen-binding (Fab)in less than 12 h. (a) Analysis of CD11b/propidium iodide (PI)-positive populations in $Fc\alpha RI_{R209L}$/FcRγ Tg mouse blood cells. The histograms show cell apoptosis in the CD11b-positive population. Tg mouse blood cells were collected 24 h after injection of 20 μg of control Fab or MIP-8a Fab in 200 μl of saline via the caudal vein. Cells were stained with fluorescein isothiocyanate (FITC) labelling anti-mouse CD11b and PI, and analysed by flow cytometry. The numbers indicate the percentage of viable cells in the CD11b-positive population. (b) Analysis of annexin V/PI double-positive populations in $Fc\alpha RI_{R209L}$/FcRγ mouse macrophage transfectants after 12 h of treatment with 10 μg/ml of control Fab or MIP-8a Fab. C, Measurement of non-apoptotic nuclei by counting hypoploid DNA. $Fc\alpha RI_{R209L}$/FcRγ mouse macrophage transfectants were incubated with 10 μg/ml of control Fab or MIP-8a Fab for 12 h. Cells were stained with PI and analysed for the appearance of hyperploid nuclei as described in Materials and methods. Numbers indicate the percentage of cells with hypoploid nuclei.

Please note: Wiley-Blackwell are not responsible for the content or functionality of any supporting materials supplied by the authors. Any queries (other than missing material) should be directed to the corresponding author for the article.